Chemical and Materials Engineering Faculty
Publications

Department of Chemical and Materials Engineering

2008

Carbon Nanoadditives to Enhance Latent Energy Storage of Phase Change Materials

Shadab Shaikh
University of Dayton

Khalid Lafdi
University of Dayton, klafdi1@udayton.edu

Kevin P. Hallinan
University of Dayton, khallinan1@udayton.edu

eCommons Citation

Carbon nanoadditives to enhance latent energy storage of phase change materials

Shadab Shaikh, Khalid Lafdi,[a] and Kevin Hallinan
University of Dayton, 300 College Park, Dayton, Ohio 45469, USA

Latent energy storage capacity was analyzed for a system consisting of carbon nanoparticles doped phase change materials (PCMs). Three types of samples were prepared by doping shell wax with single wall carbon nanotubes (SWCNTs), multiwall CNTs, and carbon nanofibers. Differential scanning calorimetry was used to measure the latent heat of fusion. The measured values of latent heat for all the samples showed a good enhancement over the latent heat of pure wax. A maximum enhancement of approximately 13% was observed for the wax/SWCNT composite corresponding to 1% loading of SWCNT. The change in latent heat was modeled by using an approximation for the intermolecular attraction based on the Lennard-Jones potential. A theoretical model was formulated to estimate the overall latent energy of the samples with the variation in volume fraction of the nanoparticles. The predicted values of latent energy from the model showed good agreement with the experimental results. It was concluded that the higher molecular density of the SWCNT and its large surface area were the reasons behind the greater intermolecular attraction in the wax/SWCNT composite, which resulted in its enhanced latent energy. The novel approach used to predict the latent heat of fusion of the wax/nanoparticle composites has a particular significance for investigating the latent heat of PCM with different types of nanoparticle additives. © *2008 American Institute of Physics*. [DOI: 10.1063/1.2903538]

I. INTRODUCTION

Among the available techniques suitable for storing thermal energy and for controlling temperature in systems subjected to periodic heating, the use of solid-liquid phase change has attracted considerable attention.[1–10] This process allows, for periodic heating, the conversion of temperature oscillations into oscillations of the melting interface and significant damping of the thermal perturbations. Phase change materials (PCMs), such as paraffin wax, exhibit desirable properties, such as high latent heat of fusion and low melting temperature, which are suitable for thermal storage applications; however, they possess a low thermal conductivity (0.15–0.3 W/m K). This relatively low value reduces the energy charge and discharge rates that are permissible during melting and solidification cycles and, therefore, limits the overall storage capacity of the PCM system. Different approaches have been used to compensate for this low thermal conductivity. One way is to design the container for the PCM such that it has a very high surface to volume ratio and it is composed of a material with a very low thermal resistance. The other way is to enhance the thermal conductivity and, hence, the heat transfer rate of the PCM by encasing the PCM within finned tubes, disperse high conductivity materials in PCM, use porous structures impregnated with PCM, and embed a metal matrix inside volume of the PCM.[11–15]

Carbon nanotubes (CNTs) with their light weight and high thermal conductivity have shown tremendous potential for heat transfer applications. The high intrinsic thermal conductivity of CNTs suggests many heat transfer enhancement applications. Much research has been reported wherein CNTs are embedded in the base fluids to increase their reactivity and improve electrical and thermal conductivity.[16,17] Recently, Elgafy and Lafdi[18] carried out a study to improve the thermal conductivity of a PCM by dispersing CNTs within the bulk of the PCM. These types of materials that are created by introducing nanoparticulates into a base material are called nanoparticle doped composites, which are a distinct form of composite materials. The process involves embedding nano- or molecular domain sized particles into organic polymers, ceramic materials, and metals. In all cases, it is perceived that the intimate inclusion of the nanoparticles in the bulk phase can completely change the properties of these base materials and can drastically add to the electrical and thermal conductivity, as well as to the mechanical strength properties of the original material.[16–18]

There is a limited amount of research that deals with the modeling of the latent heat of materials. Devireddy *et al.*[19] carried out a theoretical study on latent heat of fusion to predict the experimentally measured behavior of salt solutions during the freezing process in a differential scanning calorimetry (DSC) sample pan based on the full set of heat and mass transport equations. Recently, Garai[20] presented a model for the latent heat of fusion based on the concept of viscous drag resistance during the melting process. The author used the viscosity model to compute the latent heat from the viscosity, melting temperature, and size and mass of atoms. Apart from this work, there is no significant work in literature that deals with the modeling of latent heat of a pure solid or solids with micro- and nanoadditives. In the present work, we characterize the change in latent heat of a CNT doped PCM. For a matrix with such nanoscale particles, the

a)Author to whom correspondence should be addressed. Electronic mail: khalid.lafdi@udri.udayton.edu.

surface to volume ratio can be very high with only a small concentration of the CNTs, and consequently, the molecular interaction between the nanotube surface and the PCM can change the energy storage capacity of the system. It is hypothesized that the heat of fusion and the melting point could also be changed due to the insertion of such nanomatrix inside the PCM. In this research, experiments are conducted to show changes in latent heat that result from the inclusion of CNTs in a PCM. In addition, a simple analytical and numerical study is carried out to model the change in latent energy per unit volume of a low thermal conductivity PCM (paraffin wax) inside a nanoscale matrix. This study is based on modeling the change in the latent heat of fusion due to the CNT surface–PCM interaction. The concept was adopted from the work of Israelchvili,[21] which deals with the study of intermolecular and surface forces and their role in determining the properties of simple systems, such as gases, liquids, and solids. The theoretical model presented in this study for PCM, which is based on intermolecular attraction, is a novel approach for the analysis of latent heat of fusion, which is an important thermal property for any material undergoing phase change.

II. INTERMOLECULAR ATTRACTION AND PHASE CHANGE

Intermolecular forces are defined as forces that are exerted by molecules on each other and that, in general, affect the macroscopic properties of the bulk material comprised of the molecules. Such forces may be either attractive or repulsive in nature. They are conveniently divided into two classes: short-range forces, which operate when the centers of the molecules are separated by 3 Å or less, and long-range forces, which operate at greater distances. Generally, if molecules do not tend to chemically interact, the short-range forces between them are repulsive. Long-range forces, or van der Waals forces, are attractive and account for a wide range of physical phenomena, such as friction, surface tension, and adhesion and cohesion of liquids and solids. There is a chemical potential energy in the weak van der Waals attractions as well as in the strong ionic and covalent bonds. This chemical potential energy is, *however, a major factor in the latent energy of a material.* Collectively, the attractive and repulsive forces can be modeled by using the Lennard-Jones potential (also referred to as the LJ potential, 6–12 potential or, less commonly, 12-6 potential). The LJ potential is of the form

$$w(r) = -\frac{A}{r^6} + \frac{B}{r^{12}},\qquad(1)$$

where r is the separation between interacting molecules, (A/r^6) is the attractive contribution due to the van der Waals interaction, and (B/r^{12}) describes the repulsive contribution.

A phase change transition from solid to liquid is endothermic, e.g., a heat absorption process wherein the heat energy is used to overcome the weak intermolecular attractions. When heat is added to a substance, the energy level will increase by an amount that is governed by the specific heat capacity. However, if a change in phase takes place, the energy is used to disrupt the intermolecular forces instead of to raise the temperature. This energy required to change a gram of a substance from the solid to the liquid state without changing its temperature is commonly called its "heat of fusion." This energy breaks down the solid bonds but leaves a significant amount of energy associated with the intermolecular forces of the liquid state. For materials such as nanoparticle doped PCM, it is expected that the intimate inclusion of nanoparticles with PCM can alter these long-range forces if the concentration of the CNTs is high enough. If the CNT/wax interaction potential is greater than that between wax molecules themselves, it is plausible that the heat of fusion can be increased.

III. EXPERIMENTAL STUDY

A. Sample preparation

Three types of nanoparticle doped PCM were selected to study the change in latent energy due to the intermolecular attraction between the PCM and nanoparticle additives. The PCM used was paraffin wax (shell wax 100) with a low melting point. The three different nanoparticles used to prepare the wax/nanoparticle composite were single wall CNTs (SWCNTs), multiwall CNTs (MWCNTs), and carbon nanofibers (CNFs) with nominal diameters of about 1, 10, and 100 nm, respectively. The heat of fusion was measured for volume fractions ranging from 0.1% to 1% for each type of nanoparticle. The nanoparticle doped wax samples were subjected to shear mixing by using ultrasonic sonication for about 4 h to obtain a well dispersed suspension. The samples prepared, thus, were solidified and these were used for latent heat measurements.

B. Latent heat measurement and results

DSC was used to measure the latent heat of fusion. All of the samples were subjected to two melting-freezing cycles under similar test conditions. The variation in the measured latent heat values for the two cycles for pure wax and for different samples corresponding to each type of nanoparticle was between 1 and 2 J/g. The addition of the three types of nanoparticles with different percent loadings slightly raised the melting temperature of wax in the range of 0.4–1 °C. The latent heat values obtained for the pure shell wax and different wax/nanoparticle composites are shown in Table I. It was observed that for all of the nanoparticle types, with an increase in the percent volume fraction, the latent heat showed a reasonable increase. The greatest percentage enhancement in latent heat as compared to pure shell wax was observed for the wax/SWCNT composite (approximately 13%) corresponding to 1% volume fraction of carbon nanotubes.

The SWCNTs used for the analysis were the smallest of the nanoparticles, having a nominal diameter of about 1 nm and, hence, a large surface to volume ratio. The visual inspection of the suspensions revealed that the wax/SWCNT suspension also had better dispersion as compared to the other two types of nanoparticles. The larger surface area and greater dispersion of the smaller SWCNTs certainly resulted in a greater intermolecular attraction with the wax molecules.

TABLE I. DSC values of latent heat of wax and nanoparticle doped composites.

Sample	Latent heat (J/kg)	Enhancement (%)
Shell wax 100 (pure)	156 300	
Shell wax with SWCNT 1 nm (0.1%)	168 200	7.62
Shell wax with SWCNT 1 nm (0.4%)	170 600	9.12
Shell wax with SWCNT 1 nm (0.7%)	174 600	11.72
Shell wax with SWCNT 1 nm (1%)	176 600	12.98
Shell wax with MWCNT 10 nm (0.1%)	165 200	5.69
Shell wax with MWCNT 10 nm (0.4%)	168 000	7.48
Shell wax with MWCNT 10 nm (0.7%)	170 900	9.36
Shell wax with MWCNT 10 nm (1%)	172 100	10.08
Shell wax with CNF 100 nm (0.1%)	161 700	3.47
Shell wax with CNF 100 nm (0.4%)	163 100	4.34
Shell wax with CNF 100 nm (0.7%)	165 600	5.93
Shell wax with CNF 100 nm (1%)	166 900	6.80

Thus, the increase in the intermolecular forces within the SWCNT/wax composite would have raised its latent heat of fusion. The smaller size of the SWCNTs would also mean that their molecular density was higher than for both the MWCNT and the CNF nanocomposites. These factors could have contributed to changing the intermolecular forces and, eventually, the latent heat for the nanocomposites as compared to the pure wax.

IV. THEORETICAL STUDY

A. Model description

To model the presence of the nanoparticles in the wax, a uniform dispersion of the nanoparticles was assumed, with uniform spacing between the particles. As shown in Fig. 1, a simple two-dimensional line arrangement of CNT with diameter d is assumed. The distance between two adjacent CNTs is S. Due to symmetry, only one quarter of the shape needs to be considered.

The first step in the analysis is to calculate the intermolecular potential between a single CNT and the surrounding PCM. Consider a differential element within the CNT at angle θ and radius r with area $rdrd\theta$, as shown in Fig. 2. The
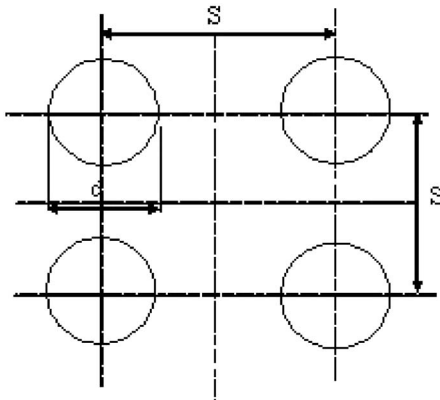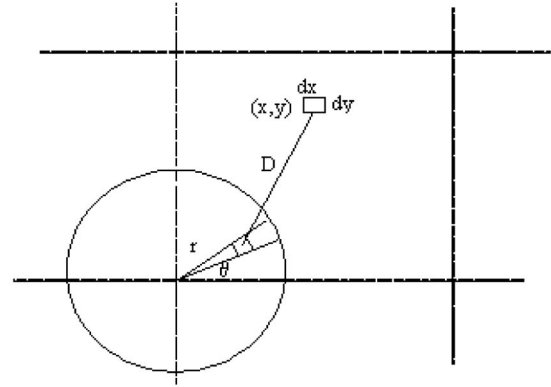

FIG. 1. CNT arrangement.

FIG. 2. Physical model for theoretical study.

number of molecules in this element can be defined as $\rho rdrd\theta$, where ρ is the molecule number density for the fiber material.

By assuming that the intermolecular potential is purely attractive between the nanoparticle and PCM molecules, the potential function can take the following form:

$$w = -c/r^n. \tag{2}$$

For van der Waals interactions, the value of n is usually taken as 6, and for charged nonpolar interactions, it is taken as 4. For the current study, the value of n was considered as 6. The value of c, which is a constant, is taken as 10^{-76} J m^6.

Based on the geometry depicted in Fig. 2, the potential energy function at any point in the PCM with coordinates (x, y) can be defined by the relation given by the integral below. The negative sign is for the attractive potential as mentioned in the work of Israelchvilli,[21]

$$w(x,y) = -\rho_{fiber}c \int_0^{\pi/2} \int_0^{d/2} \frac{rdrd\theta}{[(x - r\cos\theta)^2 + (y - r\sin\theta)^2]^3}. \tag{3}$$

The molecules of the PCM at the point (x, y) will have an attractive force directed toward the surface. This attraction can change the melting temperature or the latent heat of fusion. It was assumed that the change in latent heat of fusion for the wax/nanoparticle composite was equal to the sum of all the potential interactions between the nanoparticle and PCM molecules over the entire region of PCM. The change in latent heat of fusion was, thus, modeled as

$$\Delta H = \rho_{PCM} \int_{over} \int_{PCM} w(x,y)dxdy. \tag{4}$$

Thus, the magnitude of the change in latent heat is given by

$$\Delta H = c\rho_{\text{fiber}}\rho_{\text{PCM}} \int_{\text{over}} \int_{\text{PCM}} \left\{ \int_0^{\pi/2} \int_0^{d/2} \frac{r\,dr\,d\theta}{[(x - r\cos\theta)^2 + (y - r\sin\theta)^2]^3} \right\} dx\,dy. \tag{5}$$

Let the constant $c\rho_{\text{fiber}}\rho_{\text{PCM}}$ be represented by

$$A = c\rho_{\text{fiber}}\rho_{\text{PCM}}, \tag{6}$$

which yields the following final expression for the change in latent heat:

$$\Delta H = A \int_{\text{over}} \int_{\text{PCM}} \left\{ \int_0^{\pi/2} \int_0^{d/2} \frac{r\,dr\,d\theta}{[(x - r\cos\theta)^2 + (y - r\sin\theta)^2]^3} \right\} dx\,dy. \tag{7}$$

B. Numerical simulation

The complex integral in Eq. (3) was solved by using a numerical integration procedure using the MATLAB software. This was achieved by generating a grid for the PCM region, as shown in Fig. 3. The integration was performed at each grid point in the domain to get the values of $w(x,y)$. These values were then used to get the ratio $\Delta H/A$. Before implementing the model to compute the change in latent heat of different wax/nanoparticle composites, a grid sensitivity analysis was performed. Based on the results in Table II, in the case of the interaction between nanofiber (100 nm diameter) and wax, a grid size of 50×50 was selected for the latent heat analysis. Here, ΔH_{av} represents the average change in latent heat.

A representation of the resulting change in latent energy obtained along a diagonal is shown in Fig. 4. Thus, one can see the trend for the latent heat of fusion change (as effected by the nanoparticle) with an increase in distance from the nanoparticle surface. From the trend shown in Fig. 4, it was clear that with the increase in distance from the nanotube surface, the change in the latent heat of fusion diminishes due to the reduction in intermolecular force of attraction between the nanotube and PCM molecules as the distance along the diagonal in Fig. 2 increased.
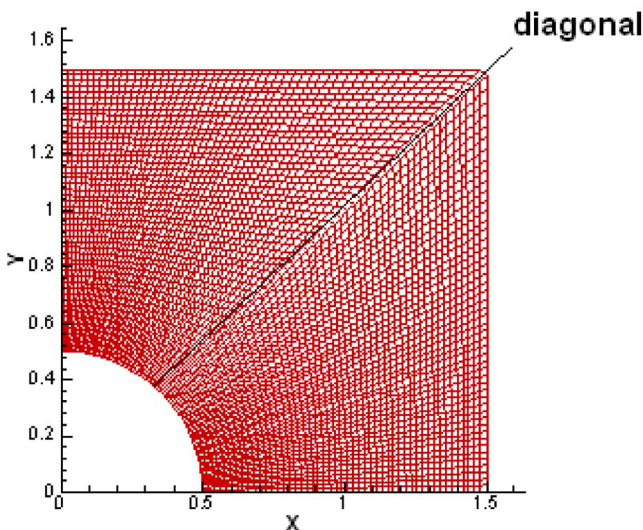

FIG. 3. (Color online) Grid shape for model domain.

C. Analysis for latent energy

To compare the overall change in latent energy of the nanoparticle doped PCM sample by using the theoretical model with experimental results for shell wax based nanocomposites, a simple study was carried out to formulate the equation for latent energy of the sample in terms of increase in volume fraction of nanotubes. Let m_{PCM} be the mass of bulk PCM without nanoparticles, m_{CNT} be the mass of nanoparticles corresponding to different percent loadings, and L be the latent heat of the PCM (shell wax). The latent energy storage for the bulk PCM is given as

$$Q_1 = m_{\text{PCM}}L. \tag{8}$$

The latent energy due to molecular interaction between the nanoparticles and the wax is given as

$$Q_{\text{mol}} = m_{\text{CNT}}\Delta H_{\text{max}}. \tag{9}$$

For ease of comparison between different types of nanoparticles of variable nominal diameters, the maximum value of change in latent heat (ΔH_{max}) from Eq. (7) was taken for each case.

The latent energy for the nanocomposite is, thus,

$$Q_2 = Q_1 + Q_{\text{mol}} = m_{\text{PCM}}L + m_{\text{CNT}}\Delta H_{\text{max}}. \tag{10}$$

The latent energy ratio, e.g., the ratio of modified latent energy due to the addition of the nanoparticles to that of the bulk phase, is given as

$$\frac{Q_2}{Q_1} = 1 + \frac{m_{\text{CNT}}}{m_{\text{PCM}}L}\Delta H_{\text{max}}. \tag{11}$$

Before plotting Eq. (11) for the latent energy ratio as a function of geometry, two important factors were taken into account. Based on the DSC measurements, it was assumed that both the increase in nanoparticle volume fraction and the type and size of the nanoparticle had a significant effect on

TABLE II. Values of change in latent heat for different grid sizes.

Grid size	ΔH_{av} (J/kg)
30×30	9143
40×40	9175
50×50	9192
60×60	9196
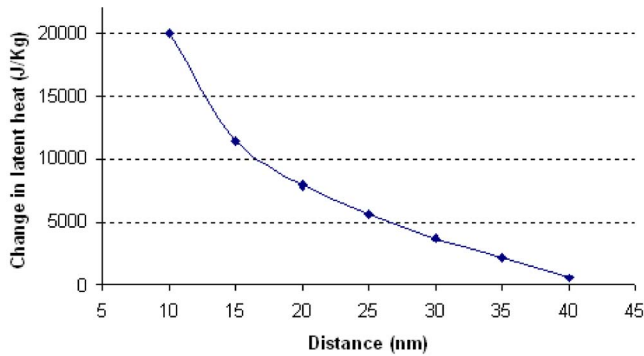
FIG. 4. (Color online) Variation of latent heat with increase in distance from nanotube surface.

FIG. 6. (Color online) Variation of molecular density constant with change in nominal diameter.

the intermolecular attraction within the mixture. Since these factors can have a net effect on the molecular density of the nanoparticles and, eventually, on their intermolecular attraction with PCM molecules, a molecular density constant was added to Eq. (6). The equation for the constant A was thus written as

$$A = C_{md} c \rho_{fiber} \rho_{PCM}. \tag{12}$$

Equation (12) was then used to calculate ΔH_{max} in Eq. (7). For each sample considered for a 0.1% nanoparticle volume fraction, the value for the molecular density constant C_{md} was determined such that the predicted value of latent energy ratio (Q_2/Q_1) from Eq. (11) matched with the experimental measured value. Thus, the constant C_{md} determined for each type of nanoparticle at a 0.1% volume fraction was then used to estimate the values of (Q_2/Q_1) for different nanoparticle volume fractions ranging from 0.2% to 1%. The value of C_{md} for each sample was then adjusted accordingly to achieve the best possible fit with the experimental results. The results for the comparison between the predicted and experimental values of (Q_2/Q_1) for the three nanoparticles are plotted as shown in Fig. 5.

The analytical model showed good agreement with the measured DSC latent energy values for all the three wax/nanoparticle composites. As observed from the plot in Fig. 5,
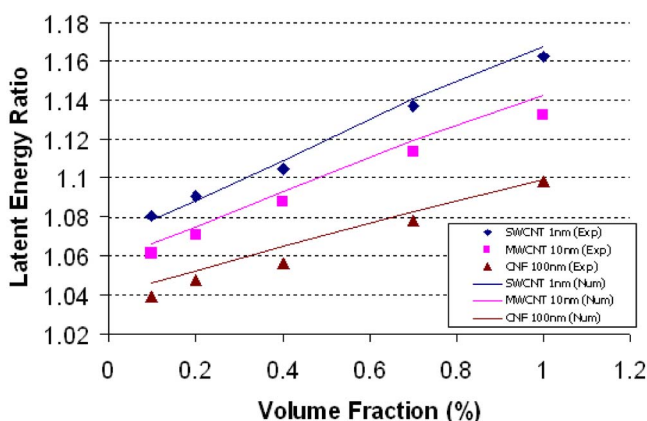
a maximum enhancement for the latent energy of just over 16% was achieved for the wax/SWCNT composite as compared to the latent energy of pure wax.

Figure 6 presents a plot for the molecular density constant as a function of nominal diameter for the three nanocomposites based on analytical predictions. The trend obtained in Fig. 6 demonstrates that the higher molecular density of the SWCNT is also a factor in the improved latent energy enhancement (in addition to greater surface area). The larger molecular density yields greater intermolecular attraction between the nanoparticles and the PCM.

V. CONCLUSIONS

An experimental and theoretical study was performed to study the change in latent energy of nanoparticle doped PCM samples. Three types of nanoparticles were prepared by doping shell wax with SWCNTs, MWCNTs, and CNFs. A maximum experimental enhancement of approximately 13% was observed for the wax/SWCNT sample corresponding to 1% loading by volume of SWCNTs. The intermolecular attraction between the molecules of nanoparticles and wax was considered as the possible reason for the enhancement of latent heat values. A theoretical study was performed to analyze the intermolecular attraction within the wax/nanoparticle composites by formulating a model for change in latent heat of fusion of wax due to interactions between nanoparticles and wax molecules by using the concept of LJ potential. A simple relation was derived for the latent energy ratio of the wax/nanoparticle composites and pure wax to compare the results from the latent heat model with experiments. The predicted values of latent energy from the model showed good agreement with the experimental results. Based on the analytical results, it was concluded that the higher molecular density of the SWCNT relative to MWCNTs and CNFs and its large surface area due to its smaller size were the reasons for a relatively larger latent energy.

The theoretical study in this work explores the LJ theory of intermolecular forces and relates it to the change in latent heat of PCM due to the inclusion of nanoparticles. The modeling technique presents a new idea and lays down a platform for a parametric study on the change in latent heat of PCM due to the addition of nanoparticles of different mate-

FIG. 5. (Color online) Comparison of predicted values for latent energy ratio with DSC experiments.

rials with different sizes, surface characteristics, and thermal properties. Most important to future developments, the analytical results provide a direction for future research for more substantial enhancement, that is, toward the development of more dense wax/nanoparticle composites with improved dispersion.

[1] W. Jianfeg, G. Yingxiu, and C. Guangming, Int. J. Energy Res. **25**, 439 (2001).
[2] S. Ahmet and K. Kamil, Energy Convers. Manage. **43**, 863 (2002).
[3] B. Gulseren and S. Ahmet, Energy Convers. Manage. **44**, 3227 (2003).
[4] G. Casano and S. Piva, Int. J. Heat Mass Transfer **45**, 4181 (2002).
[5] S. Himran, A. Suwono, and G. A. Mansoori, Energy Sources **16**, 117 (1994).
[6] K. W. Baker, J. H. Jang, and J. S. Yu, Proc. ASME/JSME Joint Thermal Engineering Conference **4**, 463 (1995).
[7] D. Pal and Y. Joshi, Numer. Heat Transfer, Part A **30**, 19 (1996).
[8] D. Pal and Y. Joshi, J. Electron. Packag. **119**, 40 (1997).
[9] E. M. Alawadhi and C. H. Amon, Proc. ITherm **1**, 289 (2000).
[10] M. J. Vesligaj and C. H. Amon, IEEE Trans. Compon. Packag. Technol. **22**, 541 (1999).
[11] R. Wirtz, A. Fuchs, V. Narla, Y. Shen, T. Zhao, and Y. Jiang, AIAA Pap. **41**, 513 (2003).
[12] S. Mauran, P. Prades, and F. L'haridon, Heat Recovery Syst. CHP. **13**, 315 (1993).
[13] X. Py, R. Olives, and S. Mauran, Int. J. Heat Mass Transfer **44**, 2727 (2001).
[14] A. D. Fedden and M. D. Franke, 9th AIAA/ASME Joint Thermophysics and Heat Transfer Conference (2006).
[15] O. Mesalhy, K. Lafdi, and A. Elgafy, Carbon **44**, 2080 (2006).
[16] J. Fukai, M. Kanou, Y. Kodama, and O. Miyatake, Energy Convers. Manage. **41**, 1543 (2000).
[17] J. Fukai, M. Kanou, Y. Kodama, and O. Miyatake, Int. J. Heat Mass Transfer **45**, 4781 (2002).
[18] A. Elgafy and K. Lafdi, Carbon **43**, 3067 (2005).
[19] V. R. Devireddy, P. H. Leo, J. S. Lowengrub, and J. C. Bischof, Int. J. Heat Mass Transfer **45**, 1409 (2002).
[20] J. Garai, Chem. Phys. Lett. **398**, 98 (2004).
[21] J. N. Israelachvili, *Intermolecular and Surface Forces* (Academic Press, San Diego, CA, 1994).